

Effect of Internal Heat Recovery in Ammonia-Water Absorption Cooling Cycles: Exergy and Structural Analysis

Dieter Boer^{1*}, Berhane Hagos Gebreslassie², Marc Medrano³, Miquel Nogués⁴

^{1,2}Department of Mechanical Engineering,
University of Rovira i Virgili, Tarragona, Spain
Phone: (+34) 977 559631
E-mail: ¹Dieter.Boer@urv.net;
²Berhane.Gebreslassie@urv.net

^{3,4}GREA Innovació Concurrent,
Universitat de Lleida Lleida, Spain
E-mail: ³mmedrano@diei.udl.cat;
⁴mnogues@diei.udl.cat

Abstract

First and second law analysis have been conducted for three low temperature driven ammonia-water absorption cooling cycles with increasing internal heat recovery. Based on the results of exergy analysis the structural analysis has been achieved. The obtained Coefficients of Structural Bonds (CSB) consider how the irreversibility of the whole cycle is affected by a change in the irreversibility related to an efficiency improvement of a single component. Trends for the different configurations are similar, while quantitative differences among the main heat exchangers are considerable. The highest values of the CSB are found for the refrigerant heat exchanger. Also the evaporator, the condenser, the generator and the absorber show values higher than unity. The lowest CSB's are obtained in the solution heat exchanger. In general, CSB's decrease with increasing efficiency. That means that for very efficient heat exchangers, a further improvement looks less attractive. The dephlegmator is an exception as it shows a singularity of the CSB value due to its complex interactions with the other components. Once the CSB's are obtained for the main components, they can be used in the structural method of the thermoeconomic optimisation. This method enables us to find the optimum design of a component in a straightforward calculation.

Keywords: Absorption cycle, ammonia-water, exergy analysis, structural analysis.

1. Introduction

Combining thermodynamics and economics, the thermoeconomic or exergoeconomic analysis can be achieved (Kotas, 1995; Bejan et al., 1996; El-Sayed, 2003). The objective of exergoeconomic optimization is the minimization of the total cost, mainly composed of capital and energy costs. In the field of refrigeration thermoeconomic analysis was applied initially to compression cycles (Wall, 1986; Dentice d'Accadia et al., 1998; Dingenç et al., 1999; Ferrer et al., 2001; Dentice d'Accadia et al., 2004; Zhang et al., 2004) and later to absorption cycles (Tozer et al., 1999; Sahin et al., 2002; Misra et al., 2003; Misra et al., 2005; Misra et al., 2006; Kizilkan et al., 2007).

One methodology used in exergoeconomic optimisation is the structural method introduced by Beyer (1970 and 1974). It is based on structural coefficients, which show how local irreversibilities in the components affect the overall irreversibility rate of the cycle. The coefficient of structural bonds (CSB) of a component k , which is obtained by variation of a parameter x_i , is defined as

$$CSB_{k;i} = \left(\frac{\partial \dot{I}_t}{\partial \dot{I}_k} \right)_{x_i = \text{var}} \quad (1)$$

where \dot{I}_k is the irreversibility rate of component k , and \dot{I}_t is the irreversibility rate of the whole cycle. Structural coefficients show how the irreversibility of the whole cycle and a single component are related. If a slight decrease in the irreversibility of one component due to an increased

efficiency causes a significant improvement in the total irreversibility of the cycle (high CSB), it will be wise to put much of the design effort in improving the efficiency of this component. Otherwise (low CSB), an improvement of the efficiency of the considered component is not worthwhile. These coefficients can help us to determine for one selected component of the system its optimum efficiency, for which a minimum total cost is achieved (Kotas, 1995).

In the present study, this method will be applied to the analysis of absorption cycles. The analysed cycles are ammonia-water absorption cooling cycles with increasing internal heat recovery. A similar approach has been applied by Sözen (2001) for an ammonia-water refrigeration cycle. Modelling starts with the first law analysis, followed by the exergy analysis (Karakas et al., 1990; Ataer et al., 1991; Best et al., 1993).

Once the irreversibilities of the components and the whole cycle are evaluated, the coefficients of structural bonds can be evaluated. Compared to a former study (Boer et al., 2005), here the CSB's are not constant, but their dependence on the efficiencies is shown and their behaviour is quantified and compared for different cycle configurations. These CSB's can be used in the structural method of exergoeconomic optimisation (Beyer, 1974). The final purpose is the design of more cost-effective absorption cycles. The application of the CSB's is described in Kizilkan et al. (2007) and will be summarized briefly. More details can be found in Kotas (1995).

The optimum efficiency specification for a component will be determined in order to obtain the minimum annual

*Corresponding author

operating cost. This operating cost is composed mainly of the fuel and capital costs.

$$C_t(x_i) = t_{op} c_{in}^e \dot{E}_{in}(x_i) + a^c \sum_{l=1}^n C_l^c(x_i) + b^c \quad (2)$$

The first term of the right hand side represents the fuel cost, the second one the capital investment amortisation and the third one other cost factors that are not affected by the optimisation, for example maintenance costs. The capital recovery factor is given by

$$a^c = \frac{i(1+i)^n}{(1+i)^n - 1} \quad (3)$$

At the optimum point

$$t_{op} c_{in}^e CSB_{k,i} \frac{\partial \dot{I}_k}{\partial x_i} = -a^c \frac{\partial C_k^c}{\partial x_i} \quad (4)$$

Equation (4) depends only on parameters of component k , which is optimised. The interaction with the system is taken into account by the CSB . $\partial \dot{I}_k / \partial x_i$ describes the effect of the efficiency parameter x_i on the irreversibility of the component. $\partial C_k^c / \partial x_i$ takes into account the dependence of the component cost on x_i . Both parameters depend on the efficiency of the analysed component. From equation (4) the efficiency that results in the lowest operating cost C_t can be obtained (Kizilkan et al., 2007).

2. Description of the cycles

For this study an ammonia-water absorption cycle has been selected (Figure 1). Basic components are the absorber (A), the condenser (C), the generator (G), and the evaporator (E). The cycle is completed by the solution heat exchanger (SHE), the dephlegmator (D) and the rectification plates (R). To obtain the necessary pressure changes, the cycles include the solution pump (P), the refrigerant expansion valve (RV) and solution expansion valve (SV).

For cycle I, the solution circulates between the absorber, where the refrigerant is absorbed at low pressure, and the generator, where the refrigerant is desorbed at high pressure (state points 1 to 6). The strong solution leaves the absorber (1), is preheated in the solution heat exchanger (3), and enters the rectification column. The column has three theoretical stages, which is sufficient in cooling applications (Roriz et al., 2003). The feed enters in central plate two. Vapour and liquid in equilibrium leave plate two towards plates one and three, respectively, while saturated liquid from plate three and saturated vapour from plate one enter plate two. Temperature and concentration of ammonia in the vapour increase from plate one to plate three. The generator acts as the reboiler of the rectification column. The weak solution (4) leaves towards the absorber. In the dephlegmator, the necessary liquid reflux is obtained, while the rest of the vapour (9) condenses completely in the condenser (10). The condensate expands in the refrigerant throttling valve, causing partial vaporisation (12), and enters the evaporator. Due to the water content of the mixture, the temperature increases during the vaporisation process as the liquid contains less and less ammonia, which is the more volatile component. Vaporisation in the evaporator is only partial, as total evaporation would

require too large of a temperature gradient. The cycle is closed when the vapour with a small liquid fraction (13) enters the absorber. Streams 15 to 22 are the external heat transfer fluids (in all cases this is water), which deliver or extract the heat to or from the cycle.

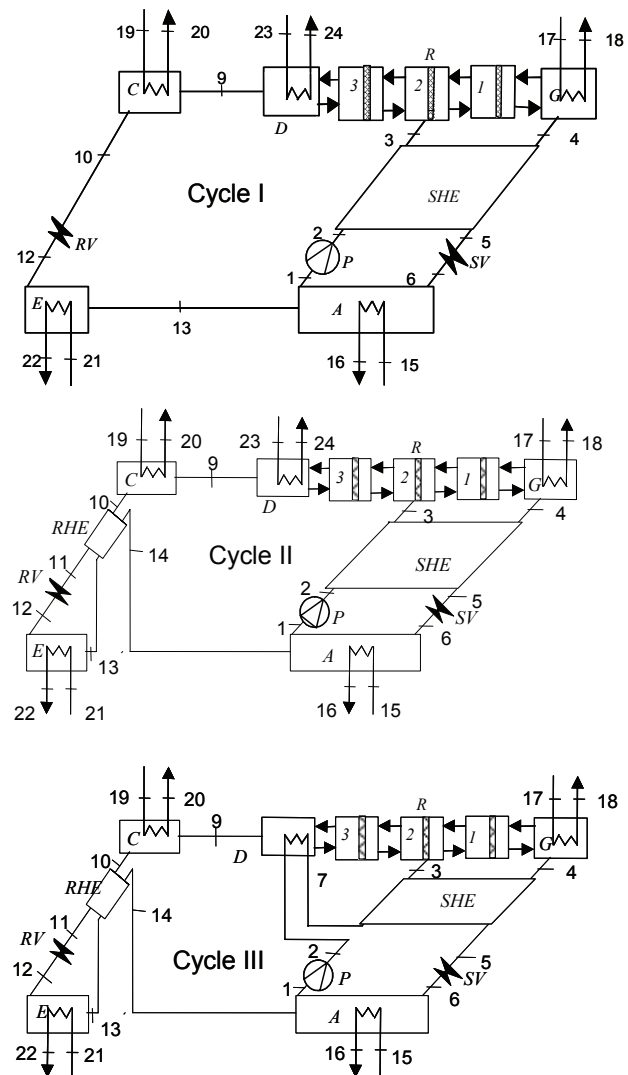


Figure 1. Ammonia-water absorption cycles with increasing internal heat recovery.

Cycle II is similar to Cycle I except for the refrigerant heat exchanger (RHE). In Cycle II after leaving the condenser the condensate (10) is subcooled (11) in order to supply heat for the partial vaporisation in the evaporator (14).

An additional feature of Cycle III is a heat exchange between the strong solution after the solution pump (2) and the dephlegmator (D). Preheating the strong solution (7) eliminates the use of cooling water in the rectifier.

3. Methodology of the simulation

A computer code for simulating the cycle has been established using the Engineering Equation Solver EES program. Properties for ammonia water are given by Tillner-Roth and Friend (1998). Typical cooling operation conditions are assumed as follows:

Evaporator cooling capacity	1000 kW
Temperatures:	
Chilled water inlet/outlet (E)	12/6°C
Cooling water inlet/outlet (parallel flow through A and C)	27°C/32°C

Hot water inlet (G)	90°C
Minimum temperature difference in the dephlegmator D	15 K
Minimum temperature difference in the rest of heat exchangers	5 K

The hot water outlet temperature in the generator is adjusted to minimise the mismatch of heat capacity rates (product of mass flow and specific heat) in the generator. This means that the temperature differences between the hot and cold streams are the same on the hot and the cold sides of the generator (Kotas, 1995). In the same way the degree of evaporation in the evaporator is chosen to obtain the same temperature difference at the inlet and outlet of the evaporator.

The main assumptions are:

- Steady state.
- Heat losses are not considered.
- Pressure losses are not considered.
- The refrigerant leaving the condensers is saturated liquid.
- The mass exchange efficiencies in absorber and generator are 0.9.
- The liquid and vapour leaving the adiabatic rectification plates are in equilibrium.
- The solution and refrigerant valves are adiabatic.
- The pump efficiency is 0.6.

Modeling starts with a first law analysis. Steady state mass and energy balances for the components of the cycles are established as follows:

Global mass balance:

$$\Sigma \dot{m}_i = \Sigma \dot{m}_e \quad (5)$$

Mass balance for ammonia:

$$\Sigma \dot{m}_i z_i = \Sigma \dot{m}_e z_e \quad (6)$$

Energy balance:

$$0 = \dot{Q} - \dot{W} + \sum_i \dot{m}_i h_i - \sum_e \dot{m}_e h_e \quad (7)$$

For adiabatic components the energy balance is:

$$\Sigma \dot{m}_i h_i = \Sigma \dot{m}_e h_e + \dot{W} \quad (8)$$

The mechanical power only appears in the energy balance of the pump. The mass exchange efficiency for absorber and generator takes into account that thermodynamic equilibrium is not totally reached at the outlet (Ataer et al., 1991) and is defined as:

$$\varepsilon_m = \frac{(z_i - z_e)_{real}}{(z_i - z_e)_{equilibrium}} \quad (9)$$

The coefficient of performance (COP) is defined by the cooling output divided by the driving heat input.

$$COP = \frac{\dot{m}_{21}(h_{22} - h_{21})}{\dot{m}_{17}(h_{18} - h_{17})} \quad (10)$$

The driving heat is delivered by the hot water. The subscripts in Eqns (10) and (16) correspond to the numeration of state points presented in Figure 1. The general exergy balance is given by Kotas (1995):

$$0 = \sum_i (1 - \frac{T_0}{T_i}) \dot{Q}_i - \dot{W} + \sum_i \dot{m}_i e_i - \sum_e \dot{m}_e e_e - \dot{I} \quad (11)$$

Considering components as adiabatic, the above equation can be simplified as

$$\Sigma \dot{m}_i e_i = \Sigma \dot{m}_e e_e + \dot{W} + \dot{I} \quad (12)$$

Specific exergy (Eq. 13) considers only the physical exergy (Jonsson et al., 2000). The chemical exergy of water and ammonia cancels out in the exergy balances as entering and leaving quantities are the same (Kotas, 1995). Mixing entropy has already been taken into account in the calculation of the entropy of the mixture.

$$e = h - h_0 - T_0(s - s_0) \quad (13)$$

The properties indicated with the subscript 0 refer to the environmental state, which is taken as 25°C and 1 bar. Using exergy flow rates

$$\dot{E} = \dot{m}e \quad (14)$$

it follows

$$\Sigma \dot{E}_i = \Sigma \dot{E}_e + \dot{W} + \dot{I} \quad (15)$$

Irreversibilities are obtained from the exergy analysis. The resulting equations for the different components are given by Karakas et al. (1990). The exergy efficiency is defined as the useful exergy output divided by the required exergy input. For the cycle the exergy input is given by the reduction of the exergy flow of the external heating fluid in the generator and the pump work. The exergy output produced in the evaporator is given by the increase in the exergy flow of the chilled water.

$$\psi = \frac{\dot{m}_{21}(e_{21} - e_{22})}{\dot{m}_{17}(e_{18} - e_{17}) + \dot{W}_{pump}} \quad (16)$$

The output data obtained are:

- The pressures, temperatures, concentrations, mass flows, enthalpies, entropies and exergies of each state point of streams.
- The thermal or, in the case of the solution pump, mechanical power and irreversibility rate of the main components.
- The COP and the exergetic efficiency.

Once the irreversibilities of the components and the whole cycle have been determined, a parametric study can be achieved. The UA values in Table 1 correspond to minimum temperature differences ΔT_{min} in the heat exchangers for the base case taken as 5 K, except for the dephlegmator, where it is 15 K. UA values for all components are maintained constant (Boer et al., 2005), except for the one which is analysed. For this selected component, the minimum temperature difference is varied, which results in a variation of UA . The variation of ΔT_{min} for any component is typically between 1 and 10 K, if operation is feasible, except for the dephlegmator where variations were achieved between 5 and 30 K. This range is limited by the operating conditions in order to avoid high solution flow ratios of operation with low performance. As a result, the influence of the heat transfer efficiency of this component on its own irreversibility and also on the irreversibility of the whole cycle is evaluated. These data can be used to determine the CSB (Eqn. 1) for a given set of

Table 1: UA Values Corresponding to the Fixed ΔT_{min} in the Base Case.

Component	Cycle		
	I	II	III
	UA [kW/K]		
A	269.2	264.3	233.4
C	144.8	136.3	136.5
G	318.5	299.8	297.6
E	131.4	131.4	131.4
D	6.2	5.9	7.3
RHE	-	6.3	6.4
SHE	254.6	239.5	229.5

operating conditions, which is the main objective of this analysis.

4. Results

4.1 First and second law analysis

Results of the energetic analysis for the different state points are presented in Table 2, 3 and 4. The corresponding thermal or mechanical power of the components are given in Table 5.

The exergy balances have been achieved for the different components in order to obtain the irreversibilities (Table 6). For all cycles, the highest irreversibilities were found in the solution heat exchanger (SHE) followed by the absorber (A), the evaporator (E) the condenser (C) and the generator (G).

The irreversibilities of the solution expansion valve (SV) and the dephlegmator (D) were less important. The irreversibility of the refrigerant expansion valve (RV) is considerably reduced by the introduction of the refrigerant heat exchanger (RHE). The refrigerant heat exchanger (RHE) and the rectification (R) contribute less to the irreversibilities. Irreversibilities in the adiabatic rectification plates were low and caused by mixing of streams with different temperatures and concentrations.

Table 2: Operating Conditions for Cycle I.

State Point	T [C]	P [bar]	z [kg kg ⁻¹]	\dot{m} [kg s ⁻¹]	h [kJ kg ⁻¹]	s [kJ kg ⁻¹ K ⁻¹]	e [kJ kg ⁻¹]	\dot{E} [kW]
1	32	4.452	0.513	9.321	72.05	1.025	27.31	254.6
2	32.6	14.29	0.513	9.321	73.27	1.025	28.7	267.6
3	74.7	14.29	0.513	9.321	273.4	1.638	46.09	429.6
4	85	14.29	0.46	8.411	299.3	1.687	57.28	481.8
5	37.6	14.29	0.46	8.411	77.43	1.026	32.64	274.5
6	37.8	4.452	0.46	8.411	77.43	1.029	31.5	264.9
9	47	14.29	0.999	0.91	1666	5.766	207.4	188.8
10	37	14.29	0.999	0.91	518	2.07	162	147.4
12	1	4.452	0.999	0.91	518	2.113	149	135.6
13	7	4.452	0.999	0.91	1617	6.119	53.48	48.67
15	27	1	0	69.434	113.3	0.395	0.028	1.939
16	32	1	0	69.434	134.2	0.464	0.338	23.48
17	90	1.702	0	38.371	377.1	1.193	26.05	999.5
18	80.1	1.702	0	38.371	335.6	1.077	19.09	732.5
19	27	1	0	49.97	113.3	0.395	0.028	1.395
20	32	1	0	49.97	134.2	0.464	0.338	16.9
21	12	1	0	39.71	50.51	0.181	1.22	48.54
22	6	1	0	39.71	25.32	0.091	2.652	105.3
23	27	1	0	5.192	113.3	0.395	0.028	0.145
24	32	1	0	5.192	134.2	0.464	0.338	1.756

Table 3: Conditions for Cycle II.

State Point	T [C]	P [bar]	z [kg kg ⁻¹]	\dot{m} [kg s ⁻¹]	h [kJ kg ⁻¹]	s [kJ kg ⁻¹ K ⁻¹]	e [kJ kg ⁻¹]	\dot{E} [kW]
1	32	4.453	0.513	8.771	72.06	1.025	27.31	239.6
2	32.6	14.29	0.513	8.771	73.28	1.025	28.7	251.7
3	74.7	14.29	0.513	8.771	273.4	1.638	46.08	404.2
4	85	14.29	0.46	7.914	299.3	1.687	57.28	453.3
5	37.6	14.29	0.46	7.914	77.44	1.026	32.64	258.3
6	37.8	4.453	0.46	7.914	77.44	1.029	31.5	249.3
9	47	14.29	0.999	0.857	1666	5.766	207.4	177.7
10	37	14.29	0.999	0.857	518	2.07	162	138.7
11	22.8	14.29	0.999	0.857	449.3	1.843	160.9	137.8
12	1	4.453	0.999	0.857	449.3	1.862	155	132.8
13	7	4.453	0.999	0.857	1617	6.118	53.48	45.81
14	32	4.453	0.999	0.857	1685	6.354	51.98	44.53
15	27	1	0	68.16	113.3	0.395	0.028	1.903
16	32	1	0	68.16	134.2	0.464	0.338	23.05
17	90	1.702	0	36.104	377.1	1.193	26.05	940.4
18	80.1	1.702	0	36.104	335.6	1.077	19.09	689.2
19	27	1	0	47.029	113.3	0.395	0.028	1.313
20	32	1	0	47.029	134.2	0.464	0.338	15.91
21	12	1	0	39.71	50.51	0.181	1.222	48.54
22	6	1	0	39.71	25.32	0.091	2.652	105.3
23	27	1	0	4.886	113.3	0.395	0.02792	0.1364
24	32	1	0	4.886	134.2	0.464	0.3382	1.652

Table 4: Operating Conditions for Cycle III.

State point	T [C]	p [bar]	z [kg kg ⁻¹]	\dot{m} [kg s ⁻¹]	h [kJ kg ⁻¹]	s [kJ kg ⁻¹ K ⁻¹]	E [kJ kg ⁻¹]	\dot{E} [kW]
1	32	4.452	0.513	8.769	72.05	1.025	27.31	239.5
2	32.6	14.29	0.513	8.769	73.27	1.025	28.7	251.7
3	74.9	14.29	0.513	8.769	274.6	1.641	46.26	405.6
4	85	14.29	0.46	7.912	299.3	1.687	57.28	453.2
5	40.1	14.29	0.46	7.912	88.75	1.062	33.14	262.2
6	40.2	4.452	0.46	7.912	88.75	1.066	32.01	253.3
7	35.1	14.29	0.513	8.769	84.7	1.062	29.03	254.6
9	47.6	14.29	0.999	0.856	1668	5.772	207.5	177.8
10	37	14.29	0.999	0.856	517.9	2.069	161.9	138.6
11	22.6	14.29	0.999	0.856	448.6	1.84	160.8	137.7
12	1	4.452	0.999	0.856	448.6	1.86	155	132.7
13	7	4.452	0.999	0.856	1616	6.117	53.48	45.8
14	32	4.452	0.999	0.856	1686	6.354	51.96	44.51
15	27	1	0	72.443	113.3	0.395	0.028	2.023
16	32	1	0	72.443	134.2	0.464	0.338	24.5
17	90	1.702	0	36.039	377.1	1.193	26.05	938.7
18	80.2	1.702	0	36.039	335.8	1.078	19.12	689.2
19	27	1	0	47.11	113.3	0.395	0.028	1.315
20	32	1	0	47.11	134.2	0.464	0.338	15.93
21	12	1	0	39.71	50.51	0.181	1.222	48.54
22	6	1	0	39.71	25.32	0.091	2.652	105.3

Table 5: Thermal or Mechanical Power for a Fixed Cooling Capacity.

Component	Cycle		
	I	II	III
	Power [kW]		
A	1451	1425	1514
C	1044	983	985
G	1593	1499	1488
E	1000	1000	1000
D	109	102	100
RHE		59	59
SHE	1866	1756	1666
P	19	18	18

Table 6: Irreversibilities.

Component	Cycle		
	I	II	III
	Irreversibility [kW]		
A	37.46	33.10	35.78
C	25.87	24.35	24.49
G	13.36	12.57	12.42
E	30.17	30.20	30.17
D	9.29	8.75	7.34
RHE	-	2.23	2.24
SHE	45.24	42.57	39.95
P	5.93	5.58	5.58
RV	11.83	5.03	4.99
SV	9.61	9.04	8.99
R	1.68	1.58	1.48

The main source of irreversibilities is the temperature between hot and cold streams. Irreversibilities for *SHE* are high due to the low generator temperature. The concentration difference between weak and strong solution is small and solution flow rates large. Results agree with Best et al. (1993), except in the generator. In our case the generator shows lower irreversibilities, as the mismatch of the heat capacity rates has been minimized.

Heat integration affected the irreversibilities in the following way. The main effect of the refrigerant heat exchanger (component *RHE* in Cycles II and III) was a strong reduction in the irreversibility of the refrigerant expansion valve due to the change in working conditions. The refrigerant valve inlet temperature (state points 10 and 11 for Cycles I and II, respectively) decreased from 37°C to about 22.8°C, thus reducing the enthalpy h_{12} in the evaporator inlet from 518 kJ/kg to about 449 kJ/kg. This led to an increase in the enthalpy difference in the evaporator and, for a fixed cooling power, the refrigerant mass flow decreased from 0.91 kg/s to 0.857 kg/s. Consequently, the solution flow rate also decreased. The reduction of the irreversibility in the refrigerant valve is greater than the irreversibility added by the refrigerant heat exchanger. The irreversibility of absorber (*A*) decreased because the vapour (14) entered with less difference in temperature with regard to the solution (6) and the mixing took place at a more uniform temperature. Because of the reduction in the mass flows, all irreversibilities were generally smaller.

The combined solution preheater and dephlegmator (component *D* in Cycle III) irreversibility in the solution heat exchanger was also reduced by preheating of the solution. The strong solution entered the solution heat exchanger at 35.1°C (T_7) compared to 32.6°C (T_2) in Cycle II. At the same time, however, T_5 increased from 37.6°C in Cycle II to 40.1°C in Cycle III, and thus increased the absorber irreversibility. Thus, the reduction of irreversibility in the dephlegmator and solution heat exchanger is partially compensated for by the increase in the absorber.

These reductions in irreversibilities due to the better heat integration improved the *COP* and the exergetic efficiencies Ψ of the cycles (Table 7). The refrigerant heat exchanger had a greater effect (+6%) than the solution preheating (compared to Cycle II less than 1%).

Table 7: Energetic (*COP*) and Exergetic Efficiencies (Ψ).

Cycle	I	II	III
<i>COP</i>	0.628	0.667	0.672
Increase of <i>COP</i> compared to Cycle I (%)	-	6.2	7.0
Ψ	0.199	0.211	0.212
Increase of Ψ compared to Cycle I (%)	-	6.0	6.5

4.2 Grassmann diagrams

The exergy flows and irreversibilities can be represented in graphical form. The Grassmann diagram (Szargut et al., 1988; Kotas, 1995) can be used to illustrate cyclic processes and their components with their corresponding irreversibilities, the exergy flows and the recirculation of exergy in the cycle. The inlet exergy flow is on one side of each component, and in the component itself, part of this exergy flow is degraded due to irreversibilities. On the other side of the component exergy flows are leaving. Each component represents a graphical exergy balance and shows how part of the exergy input is lost in the successive energy transformation in the cycles. The widths of the lines are proportional to their exergy flow. This type of diagram already has been employed for absorption cycles (Anand et al., 1984; Szargut et al., 1988; Jeong et al., 2003). The thermal exergy flows E^Q correspond to the change in the exergy flow rate of the external fluids.

Figure 2 represents the exergy flows of Cycle I. The description starts with the external heat and exergy transfer. The exergy input E^Q_G represents the reduction in hot water exergy and the exergy output E^Q_E represents the increase in chilled water exergy. The exergy flows E^Q_A , E^Q_C and E^Q_D are dissipated by the cooling water.

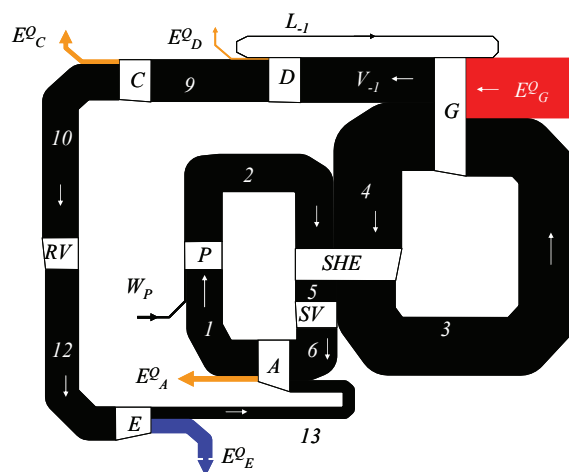


Figure 2. Grassmann diagrams of Cycle I.

With regard to the cycle itself, on the right side is situated the solution circuit with the strong solution (points 1 to 3) and the weak solution (points 4 to 6). The exergy input to the cycle is given by the thermal exergy E^Q_G supplied to the generator and the pump work W_P . This exergy is used to increase the exergy of the solution (points 3 to 4) and generate vapour flow V_{-1} . In the dephlegmator thermal exergy E^Q_D is dissipated and a reflux L_{-1} is created. In Figures 2, 3 and 4 the exergy destruction in the rectifier is included in the exergy destruction in the generator and the dephlegmator in order to simplify the figure. The vapour (point 9) enters the condenser, where again thermal

exergy E^Q_C is dissipated. The refrigerant passes through the refrigerant expansion valve and enters the evaporator, where the useful thermal exergy output E^Q_E is produced. The vapour (point 13) enters the absorber, where the refrigerant joins the solution circuit and the thermal exergy E^Q_A is dissipated. The strong solution exergy is increased in the solution heat exchanger (points 2 to 3) while the weak solution exergy is reduced (points 4 to 5). It can also be observed that the irreversibilities in the solution pump and solution expansion valve are relatively small.

In the Grassmann diagram for Cycle II (Figure 3), the refrigerant heat exchanger has been added. A new loop for the refrigerant flow is therefore added on the left hand side. The lines representing the exergy flows are slightly narrower than for Cycle I due to the reduction in the mass flows. In the Grassmann diagram for Cycle III (Figure 4), the cooling of the dephlegmator by cooling water is replaced by a heat exchange, which preheats the strong solution. The dissipation of the thermal exergy flow E^Q_D is therefore eliminated. The vapour flow V_{-1} and the strong solution 2 should enter on the same side but in order to obtain a clearer presentation an exception has been made in this case.

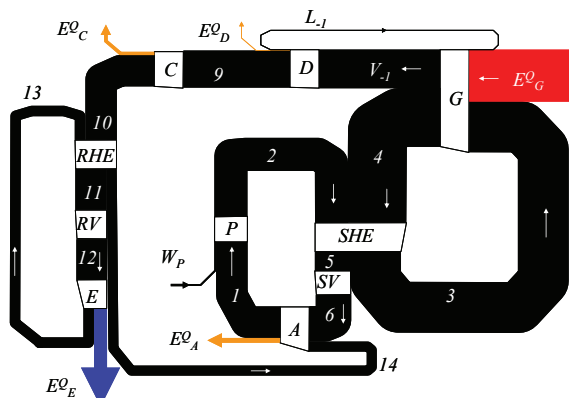


Figure 3. Grassmann diagrams of Cycle II.

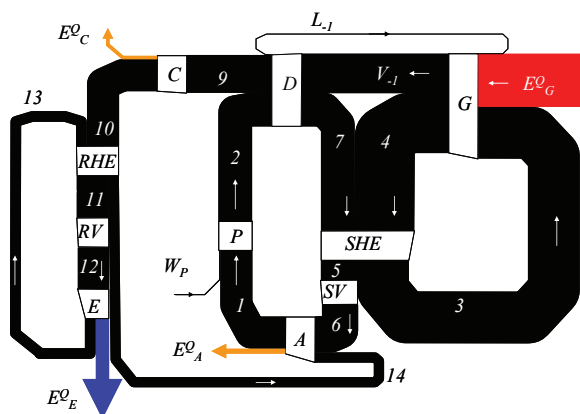


Figure 4. Grassmann diagrams of Cycle III.

4.3 Structural analysis

Once the irreversibilities are obtained, it can be checked how a change of the irreversibility of one component affects the rest of the cycle. In the component, where the minimum temperature difference is modified, the irreversibility increases with a higher minimum temperature difference. For the other components the irreversibilities

can increase or decrease depending on the interactions among the components.

The analysis starts with the absorber. The minimum temperature difference $\Delta T_{A,min}$ between solution and cooling water is modified. In Figure 5 can be observed how the irreversibility of the absorber and of the other components are affected. As $\Delta T_{A,min}$ increases, the concentration difference between weak and strong solution decreases. In order to maintain the cooling capacity, the solution flow rate has to increase. As a direct consequence, the irreversibilities in the solution heat exchanger, the generator, the solution valve and the pump increase. This effect is more accentuated at temperature differences above 5 K, in which case as the absorber $\Delta T_{A,min}$ increases the irreversibility of all components increases. Figure 5 also shows that the irreversibilities of the absorber and solution heat exchanger are the main contributors to the total irreversibility, followed by the evaporator and condenser.

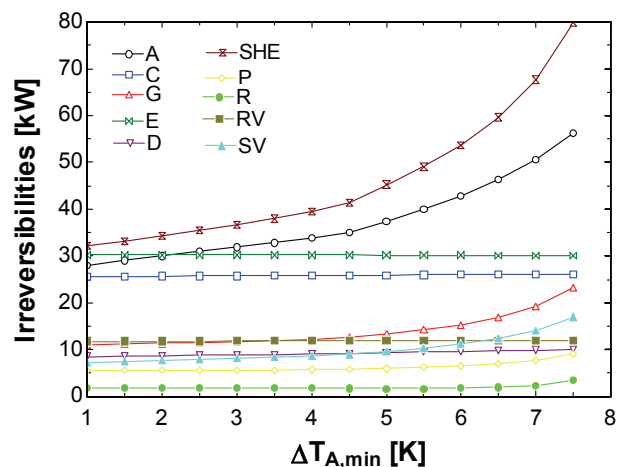


Figure 5: Irreversibilities due to a variation of absorber minimum temperature difference for Cycle I.

Figure 6 presents the total irreversibility of the whole cycle versus the irreversibility of the absorber due to the variations of ΔT_{min} for the cycle configurations considered. The trends for the different cycle configurations are similar, although there are slight differences among the values and slopes of the curves.

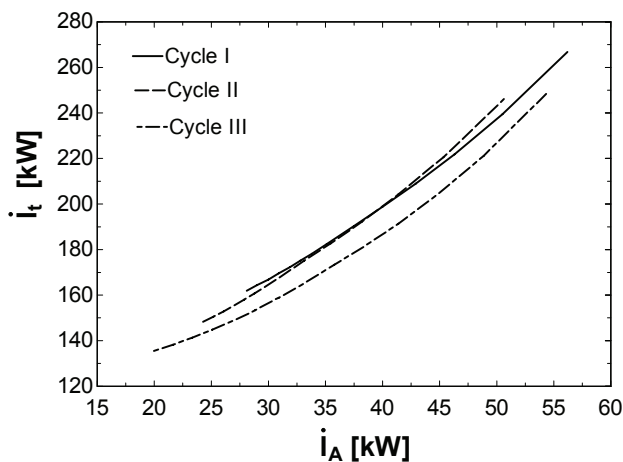


Figure 6: Total irreversibility change versus absorber irreversibility for change of absorber minimum temperature difference.

These observations will be quantified by the CSB's as they correspond to the slope of the curves representing the

total irreversibility versus the irreversibility of the absorber. Their values are determined by application of Eqn. 1. For the absorber case, such an equation can be rewritten as:

$$CSB_{A;\Delta T_A} = \left(\frac{\dot{\Delta I}_t}{\dot{\Delta I}_A} \right)_{\Delta T_{A,\min}=\text{var}, UA(\text{comp}\neq A)=\text{const}} \quad (9)$$

Values of the CSB for the absorber for the three configurations cycles are presented in *Figure 7*. At higher ΔT_{\min} the CSB 's are higher. This means that the benefit of increasing the efficiency of a less efficient heat exchange is higher than for an already efficient heat exchanger with a low ΔT_{\min} . If the value of the CSB is lower than one, the reduction of the irreversibility of the component under consideration is offset by an increase in the irreversibility of the other components. This means that a further improvement of this component is not worthwhile. Cycles I and II have very similar values of CSB 's, while cycle III has lower CSB 's for minimum temperature differences below 6 K. In the considered range CSB values are between 1.7 and 4.5. This means that in all cases a reduction in the irreversibility of the absorber is accompanied by a greater reduction in the cycle's total irreversibility. The change in the slope at a ΔT_{\min} of about 4.5 K corresponds to the point where the ΔT_{\min} shifts from the hot to the cold side of the heat exchanger. The same phenomenon explains also sudden shifts in the slopes of the CSB 's for other components. Once the dependence of the CSB 's of the component efficiencies are obtained, we can apply Eqn. 4 to determine the optimum efficiency, which results in the lowest operating cost.

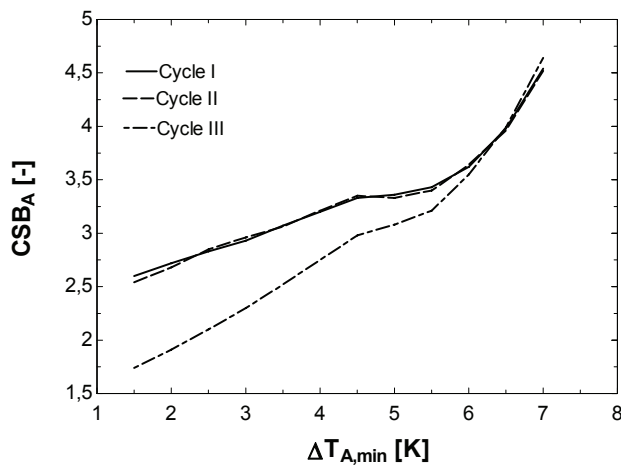


Figure 7: CSB for the absorber.

The same procedure is applied to the other main components of the different cycles in order to obtain the corresponding CSB 's (

Figure 8). Comparing the different configurations, very similar values for cycles I and II are found, while values for cycle III are generally slightly higher.

Comparing the different components, the highest CSB results are for the refrigerant heat exchanger. Even at small temperature differences values are still much higher than unity. The condenser and evaporator have similar CSB 's with values above two. For the generator and solution heat exchanger it seems less interesting to improve their heat transfer efficiencies once ΔT_{\min} is below 5 K, as in this range CSB 's are near unity. The dephlegmator shows a totally different behaviour with a singularity. While at

minimum temperature differences above 15 K CSB 's are negative, they change to positive values for lower ΔT_{\min} . This means that we should operate at a ΔT_{\min} between 10 to 15 K. For lower ΔT_{\min} the CSB approaches zero and further improvement makes no sense. These different tendencies are due to the strong interactions of the dephlegmator with the rest of the cycle. As the heat exchange efficiency improves the leaving ammonia becomes more pure, but there is an increase in other parameters, namely the heat which has to be dissipated, the temperature difference along the rectification column, and the reflux.

The interactions between the different components can be better understood observing the changes in the irreversibilities in detail. *Table 8* represents the effect of the improvement of one component on the irreversibility of the other components for the three cycle configurations. For each component changes in irreversibilities are presented in two columns, the left in kW and the right in %. The values correspond to the differences of the irreversibility for ΔT_{\min} of 1 K and 5 K, except for the dephlegmator (5 K and 30 K). A positive number represents an improvement, which is a reduction in irreversibility. Moreover, there is also a positive interaction if the reduction in the irreversibility of one component also causes a reduction in the irreversibility of other components. A grey background marks the effect on the component itself. A bold number indicates an important improvement (>10%), while an italic number corresponds to strong losses (>10%).

The reduction of the ΔT_{\min} of all main components (absorber, generator, evaporator and condenser) affects the pressures and concentrations and leads to a reduction in the solution mass flow ratio. As a consequence, the irreversibility of the solution heat exchanger SHE is always reduced. This also benefits other components of the solution circuit such as the pump P and the solution expansion valve SV .

An improvement of the absorber A reduces the solution flow rate and irreversibilities of all components in the solution circuit, including the rectification column and the generator. The same effect occurs with the condenser. As its ΔT_{\min} decreases, the high pressure of the cycle is reduced and the solution leaving the generator is weaker in ammonia. The irreversibilities in all components except the absorber are reduced.

The irreversibility is given by the difference between exergy input and exergy output. For the absorber we obtain (for Cycle I):

$$\dot{I}_A = [\dot{E}_6 + \dot{E}_{13} - \dot{E}_1] - [\dot{E}_{16} - \dot{E}_{15}] \quad (17)$$

As the heat dissipation increases, the amount of exergy output $[\dot{E}_{16} - \dot{E}_{15}]$ through the cooling water increases. As the solution flow rate increases, higher exergy flow rates of the solution circuit are obtained. But the exergy of the leaving strong solution \dot{E}_1 increases more than the exergy of the entering weak solution \dot{E}_6 . So, the exergy input $[\dot{E}_6 + \dot{E}_{13} - \dot{E}_1]$ becomes smaller. Consequently the irreversibility of the absorber decreases.

If in the generator ΔT_{\min} decreases the weak solution outlet temperature increases for a fixed hot source temperature. Also, the temperature difference along the rectification column and its irreversibility increases. On the other hand, the component for which a decrease in

irreversibility results in a decrease in irreversibilities in all weak solution becomes weaker in ammonia and the solution flow rate decreases, which in general decreases the irreversibility of the other components of the solution circuit.

In the evaporator case, a reduction in the ΔT_{min} increases the refrigerant temperature for given temperatures of the chilled water. The low pressure of the cycle and as a consequence the strong solution concentration of ammonia

in the absorber will increase. Due to the higher driving forces for the mass transfer the irreversibility of the absorber increases. The irreversibility of the rectification column increases as the irreversibility on the first plate above the generator mixes liquid and vapour with a higher concentration difference. The irreversibilities for the other components of the solution circuit decrease as the solution flow rate decreases.

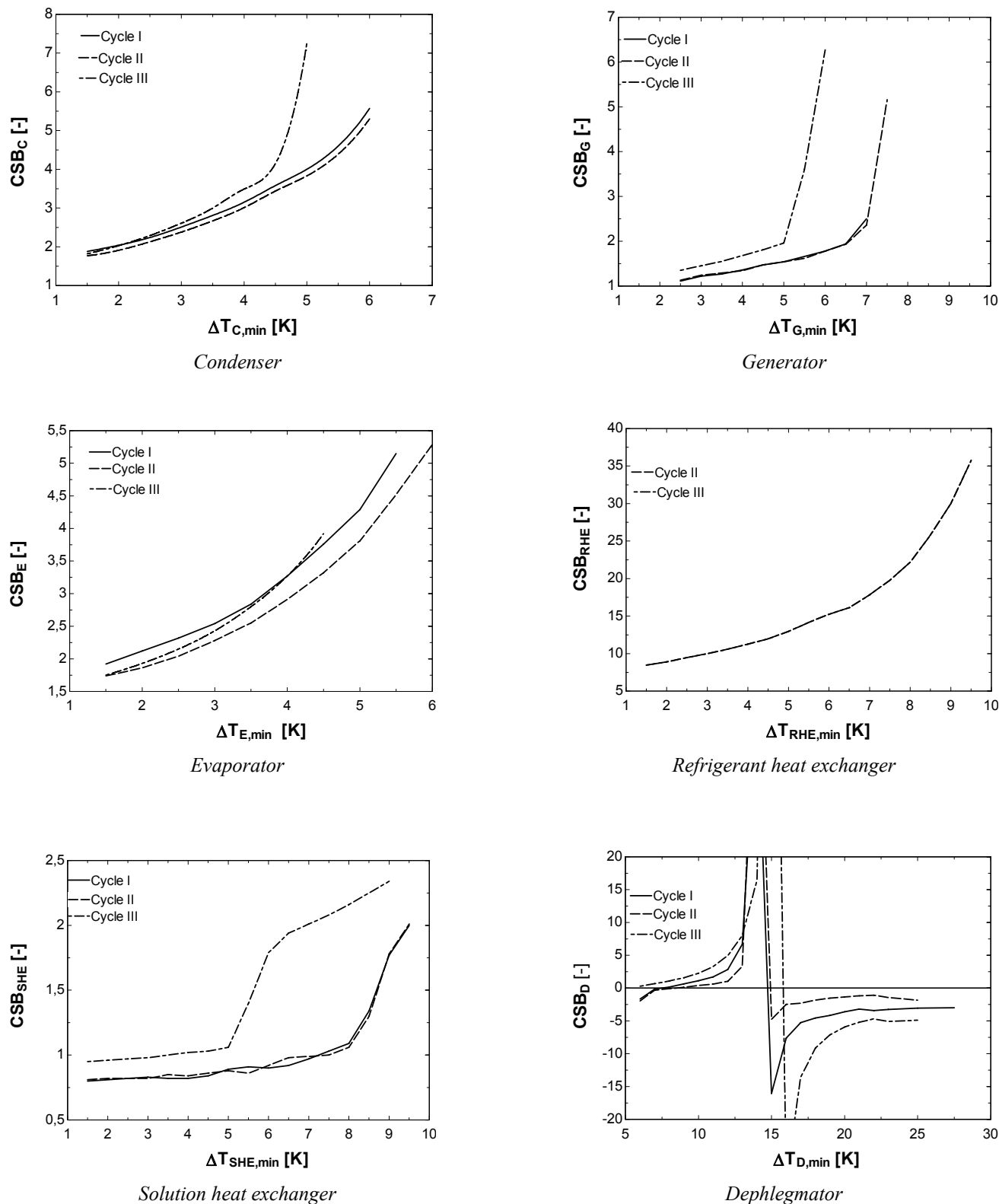


Figure 8: CSB for the main components.

Table 8: Interactions Between Components (Values Correspond to the Differences of the Irreversibility for ΔT_{min} of 1K and 5K, Except the Dephlegmator (5K And 30K)).

on the irreversibility of		Effect of the improvement of											
		A		C		G		E		RHE		SHE	
		kW	%	kW	%	kW	%	kW	%	kW	%	kW	%
Cycle I	R	-0.2	-12	-0.1	-4	-0.3	-16	-0.3	-16			0.2	13
	A	9.4	25	-8.9	-24	-4.9	-13	-5.6	-15			-2.9	-8
	C	0.3	1	12.6	49	-0.2	-1	0.6	2			-0.4	-2
	G	2.3	17	4.3	32	12.3	92	3.5	26			4.1	31
	E	0	0	0.1	0	0	0	15.6	52			0.1	0
	D	0.8	9	0.8	8	-0.7	-7	1.2	13			-1.3	-14
	RHE												
	SHE	13.1	29	14.8	33	6.8	15	20.2	45			16.2	36
	P	0.4	7	3.4	57	1.4	24	1.1	19			-0.4	-8
	RV	0	0	2.5	21	0	0	2.5	21			0	0
	SV	2.4	25	3.6	37	1.5	16	3.7	39			-2.1	-22
Cycle	28.5	15	33	17	15.9	8	42.3	22			13.3	7	
Cycle II	R	-0.2	-12	-0.1	-4	-0.3	-16	-0.2	-16	0	-0.1	0.2	13
	A	8.8	27	-8.6	-26	-4.6	-14	-6.2	-19	0	0.1	-2.7	-8
	C	0.2	1	11.8	48	-0.2	-1	0.2	1	0.4	1.5	-0.4	-2
	G	2.2	17	3.8	30	11.6	92	3	24	0.4	3.2	3.9	31
	E	0	0	0.1	0	0	0	15.6	52	0	0	0.1	0
	D	0.8	9	0.7	8	-0.6	-7	1	12	0.1	0.7	-1.3	-14
	RHE	0	1					0.6	25	0.4	15.9		
	SHE	12.3	29	13.6	32	6.4	15	18.6	44	0.9	2.2	15.3	36
	P	0.4	7	3.2	56	1.3	24	1	17	0.1	2.3	-0.4	-7
	RV	0	-1	1.1	21	0	0	0.8	17	0.7	13.4	0	1
	SV	2.3	25	3.3	36	1.4	16	3.4	38	0.2	1.9	-2.1	-22
Cycle	26.7	15	29.3	17	15.1	9	37.7	22	3.2	1.8	12.7	7	
Cycle III	R	-0.7	-44	-0.1	-4	-0.2	-15	-0.2	-13	0	0.3	0.3	19
	A	15.8	44	-6.1	-17	-3	-8	-2.7	-8	0.2	0.5	-0.6	-2
	C	0.9	4	11.6	47	-0.3	-1	0	0	0.4	1.5	-1.3	-4
	G	2.5	20	4	32	11.5	93	3	25	0.5	3.8	3.8	31
	E	-0.1	0	0.1	0	0	0	15.6	52	0	0	0.1	0
	D	0.4	5	1.1	15	-0.3	-4	1.5	21	0.1	0.8	-0.6	-8
	RHE	0.1	5			0	-1	0.5	24	0.4	16	-0.1	-3
	SHE	15.6	39	13.7	34	7.5	19	18.3	46	1.2	2.9	14.2	36
	P	0.2	4	3.1	55	1.3	24	0.8	15	0.1	2.4	-0.3	-5
	RV	-0.1	-2	1.1	22	0	1	0.9	17	0.7	13.5	0.1	1
	SV	3.3	37	3.5	39	1.6	18	3.8	42	0.2	2	-1.6	-18
Cycle	38	22	32.5	19	18.2	11	41.6	24	3.6	2.1	14	8	

A component for which a decrease in irreversibility results in a decrease in irreversibilities in all components is the refrigerant heat exchanger. Not only is this component's irreversibility reduced if ΔT_{min} is reduced, but also there is a considerable reduction in the irreversibilities of the refrigerant valve and solution heat exchanger. One way to explain this effect is that for a fixed cooling demand, if the refrigerant heat exchanger is more efficient, the enthalpy of the refrigerant entering the evaporator becomes lower, while the evaporator exit enthalpy remains constant. Therefore a lower refrigerant mass flow is needed for a given cooling power. This induces a reduction in all mass flows in the cycle. As a consequence, a strong reduction in the solution heat exchanger irreversibility is found. These high values of *CSB* appear both for Cycles II and III. As the thermal power of the refrigerant heat exchanger is only small, its effect on the total irreversibility remains limited to 7 to 8 %.

The improvement of the solution heat exchanger in Cycle I and II has a small impact on the other components except the generator and the rectification column due to the increase of the solution temperature entering the

rectification plates. This is reflected by lower *CSB* values than in Cycle III.

In general strong interactions between the components can be observed, which in general cannot be quantified easily. Since *CSB* values depend on the components, their interactions with the rest of the cycle and the operating conditions, their use simplifies exergy analyses as direct positive or negative interactions can be found observing the value of the *CSB*'s. It can be concluded that the *CSB*'s are helpful parameters, which enable us to better understand the behaviour of absorption cycles and offer a possibility to gain more insight in the thermodynamics of absorption cycles. Furthermore they can be used in economic optimisation.

5. Conclusions

Energy, exergy and structural analyses have been achieved for different configurations of ammonia-water absorption cooling cycles. The exergy analysis determines the irreversibilities of the different components and the whole cycle. But irreversibilities alone do not indicate how to improve the cycle in order to obtain the largest benefit.

To do so, the structural analysis using the coefficients of structural bonds (*CSB*) is applied. The *CSB*'s indicate how the irreversibility change in one component affects the rest of the system. This analysis includes a variation of the minimum temperature difference ΔT_{min} or *UA*-value of one component, while the *UA*-values of the other components are fixed. In this way, the effect on the irreversibility change in all the considered components of the whole cycle can be quantified by the *CSB*'s. They are different for each component and cycle configuration and also vary with the ΔT_{min} or *UA*-value.

Results show, as expected, that it is more beneficial to improve less efficient components with high ΔT_{min} or low *UA*-values rather than components which already operate with low ΔT_{min} . The components with the highest impact on the cycle as a whole are identified, and the refrigerant heat exchanger has the highest *CSB* values. Values which are in general significantly higher than unity can be seen in the evaporator, the condenser, the generator and the absorber. Values around unity are found for the solution heat exchanger. The dephlegmator shows a different behavior due to its strong interactions with the rest of the cycle. Differences between the cycle configurations are generally small.

In summary, once the exergy balances for a cycle have been established and the irreversibilities have been obtained, the structural method presents a useful method for better understanding and quantifying the interactions in the cycle. With the *CSB*, the most cost-effective cycle for a given set of operating parameters can be obtained. However, as is presented in Eqn. 8 the optimum efficiency values of each component depend also on the energy cost and the capital investment and the annual operation time.

Acknowledgements

This research project was financially supported by the "Ministerio de Ciencia y Tecnología – Dirección general de investigación" of Spain (DPI2002-00706).

Nomenclature

a^c	Capital recovery factor (-)
b^c	Part of the annual operation cost which is not affected by the optimisation (€)
c_{in}^e	Unitary cost of input exergy (€/kWh)
$c_{k,i}^l$	Unit cost of irreversibility (€/kWh)
C_l^c	Capital cost of the component l (€)
C_t	Annual operation cost (€)
<i>COP</i>	Coefficient of performance (-)
<i>CSB</i>	Coefficients of structural bonds (-)
e	Specific exergy (kJ kg ⁻¹)
\dot{E}	Exergy flow (kW)
\dot{E}_{in}	Input exergy flow (kW)
h	Specific enthalpy (kJ kg ⁻¹)
i	Interest rate (-)
\dot{I}	Irreversibility (kW)
\dot{m}	Mass flow (kg s ⁻¹)
n	Years of repayment
p	Pressure (bar)
s	Specific entropy (kJ kg ⁻¹ K ⁻¹)
t_{op}	Annual operation time (h)

T	Temperature (°C or K)
UA	Product of heat transfer coefficient and heat transfer area (kW/K)
\dot{W}_{pump}	Pump power (kW)
x_i	Parameter in the efficiency variation of the <i>CSB</i>
z	Mass fraction of ammonia (kg/kg)

Greek letters

ΔT_{min}	Minimum temperature difference in a heat exchanger (K)
$\xi_{k,i}$	Capital cost coefficient (€/kW)
Ψ	Exergetic efficiency of the cycle (-)

Subscripts

i	inlet
e	exit
k	component k
t	total
0	environmental state (25°C, 1 bar)

Components

A	Absorber
C	Condenser
D	Dephlegmator
E	Evaporator
G	Generator
P	Solution pump
R	Adiabatic rectification plates
RHE	Refrigerant heat exchanger
RV	Refrigerant expansion valve
SHE	Solution heat exchanger
SV	Solution expansion valves

References

- Anand, D. K., K. W. Lindler, et al., 1984. "Second-Law Analysis of Solar-Powered Absorption Cooling cycles and systems," *J. Solar Energy Eng* 106: 291-298.
- Ataer, E. and Y. Göğüs, 1991. "Comparative study of irreversibilities in an aqua-ammonia absorption refrigeration system." *International Journal of Refrigeration* 14(2): 86-92.
- Bejan, A., G. Tsatsaronis, et al., 1996. *Thermal Design & Optimization*. New York, John Wiley & Sons Inc.
- Best, R., J. Islas, et al., 1993. "Exergy Efficiency of an Ammonia-Water Absorption System for Ice Production." *Applied Energy* 45: 241-256.
- Beyer, J., 1970. Structural analysis- necessary part of efficiency analysis of thermal systems [Strukturuntersuchungen- notwendiger Bestandteil der Effektivitätsanalyse von Wärmeverbrauchersystemen]. *Energie-anwendung* 19(12): 358-361.
- Beyer, J., 1974. "Structure of thermal systems and economical optimisation of system parameters [Struktur wärmetechnischer Systeme und ökonomische Optimierung der Systemparameter]." *Energieanwendung* 23(9): 274-279.
- Boer, D., M. Medrano, et al., 2005. "Exergy and structural analysis of an absorption cooling cycle and the effect of efficiency parameters." *International Journal of Thermodynamics* 8(4): 191-198.
- Dentice d'Accadia, M. and F. de Rossi, 1998. "Thermoeconomic optimization of a refrigeration plant." *International Journal of Refrigeration* 21(3): 42-54.

- Dentice d'Accadia, M. and L. Vanoli, 2004. "Thermoeconomic optimisation of the condenser in a vapour compression heat pump." *International Journal of Refrigeration* 27(4): 433-441.
- Dingeç, H. and A. Ileri, 1999. "Thermoeconomic optimization of simple refrigerators." *International Journal of Energy Research* 23(11): 949-962.
- El-Sayed, Y. M., 2003. *The Thermoeconomics of energy conversions*. Amsterdam Boston.
- Ferrer, M. A., M. A. Lozano, et al., 2001. "Thermoeconomics applied to Air-Conditioning Systems." *ASHRAE Transactions AT-01-9-2*.
- Jeong, J., K. Saito, et al., 2003. *Optimum design method for a single effect absorption refrigerator based on the first and second law analysis*. 21st IIR International Congress of Refrigeration, Washington, DC (USA).
- Jonsson, M. and Y. Jinyue, 2000. "Exergy and Pinch Analysis of Diesel Engine Bottoming Cycles with Ammonia-Water Mixtures as Working Fluid." *Int.J. Applied Thermodynamics* 3(2): 57-71.
- Karakas, A., N. Egrican, et al., 1990. "Second law analysis of solar absorption-cooling cycles using Lithium Bromide/Water and Ammonia/Water as Working Fluids." *Applied Energy* 37: 169-197.
- Kizilkan, Ö., A. Sencan, et al., 2007. "Thermoeconomic optimization of a LiBr absorption refrigeration system." *Chemical Engineering and Processing: Process Intensification* 46(12): 1376-1384.
- Kotas, T., 1995. *The Exergy Method of Thermal Plant Analysis*. Melbourne, Florida, Krieger Publishing Company.
- Misra, R. D., P. K. Sahoo, et al., 2003. "Thermoeconomic optimization of a single effect water/LiBr vapour absorption refrigeration system." *International Journal of Refrigeration* 26(2): 158-169.
- Misra, R. D., P. K. Sahoo, et al., 2005. "Thermoeconomic evaluation and optimization of a double-effect H₂O/LiBr vapour-absorption refrigeration system." *International Journal of Refrigeration* 28(3): 331-343.
- Misra, R. D., P. K. Sahoo, et al., 2006. "Thermoeconomic evaluation and optimization of an aqua-ammonia vapour-absorption refrigeration system." *International Journal of Refrigeration* 29(1): 47-59.
- Roriz, L. and A. Mortal, 2003. *Study on distillation solutions for a solar assisted absorption heat pump*. Eurotherm seminar 72: Thermodynamics, heat and mass transfer of refrigeration machines and heat pumps, Valencia, Spain, Ed. Pub. IMST-UPV.
- Sahin, B. and A. Kodal, 2002. "Thermoeconomic optimization of a two stage combined refrigeration system: a finite-time approach." *International Journal of Refrigeration* 25(7): 872-877.
- Szargut, J., D. Morris, et al., 1988. *Exergy Analysis of Thermal, Chemical, and Metallurgical Processes*.
- Sözen, A., 2001. Effect of heat exchangers on performance of absorption refrigeration systems. *Energy Conversion and Management* 42(14): 1699-1716.
- Tillner Roth, R. and D. Friend, 1998. A Helmholtz Free Energy Formulation of the Thermodynamic Properties of the mixture {Ammonia + Water}. *J.Phys.Chem.Ref.Data* 27(1): 63-96.
- Tozer, R. and M. A. Lozano, 1999. *Thermo-economic optimisation of a single effect absorption chiller and cooling tower*. International Sorption Heat Pump Conference. Munich: ZAE Bayern.
- Wall, G., 1986. "Thermoeconomic Optimization of a Heat-Pump System." *Energy* 11(10): 957-967.
- Zhang, G. Q., L. Wang, et al., 2004. "Thermoeconomic optimization of small size central air conditioner." *Applied Thermal Engineering* 24(4): 471-485.